Trends in Computational and Applied Mathematics

Stable Bi-Maps on Surfaces and Their Graphs

C. MENDES DE JESUS[1], E. BOIZAN BATISTA[2] and J. C. F. COSTA[3*]

ABSTRACT. In this paper we study stable bi-maps $F = (f_1, f_2) : M \to \mathbb{R} \times \mathbb{R}^2$ from a global viewpoint, where M is a smooth closed orientable surface and $f_1 : M \to \mathbb{R}$, $f_2 : M \to \mathbb{R}^2$ are stable maps. We associate a graph to F, so-called $\mathscr{R}\mathscr{M}$-graph and study its properties. The $\mathscr{R}\mathscr{M}$-graph captures more information about the topological structure of M than other graphs that appear in literature. Moreover, some graph realization theorems are obtained.

Keywords: Stable maps, $\mathscr{R}\mathscr{M}$-graphs, closed surfaces.

1 INTRODUCTION

The graph theory has been increasingly used to solve various real-world problems, beyond, of course, the Mathematics problems. The graph theory has applications in Optimization (logistic and transportation problems), Organic Chemistry, Physics (statistical mechanics and solid state Physics), Electrical Engineering (communication network and Coding theory), among others. We can find a wide scope of these applications in the references [5, 14]. Some recent applications of graph theory include genome sequencing, starlight interferometer program and DNA sequence. The special class of bipartite graphs that will appear in this paper has many interesting and even surprising applications (see for instance [16]).

In Singularity theory, many works resort to graph theory to describe local/global invariants and combinatorial models to investigate the recognition and classification problem involving maps or map germs. The authors themselves of this paper have some works in this direction (see, for instance, [3, 8]). It is important to highlight that the Singularity theory has many practical applications in Physics, Engineering, Thermodynamic, among others.

*Corresponding author: João Carlos Ferreira Costa – E-mail: joao.costa@unesp.br

[1]Departamento de Matemática, Universidade Federal de Juiz de Fora, Via Local, 880, São Pedro, 36036-900, Juiz de Fora, MG, Brazil – E-mail: cmendesjesus@ufjf.br http://orcid.org/0000-0002-1050-2712

[2]Centro de Ciências e Tecnologia, Universidade Federal do Cariri, 63048-080, Juazeiro do Norte, CE, Brazil – E-mail: erica.batista@ufca.edu.br https://orcid.org/0000-0003-0125-9949

[3]Departamento de Matemática, Universidade Estadual Paulista (UNESP), 15054-000, São José do Rio Preto, SP, Brazil – E-mail: joao.costa@unesp.br https://orcid.org/0000-0002-0428-4640

In this work, we resort graphs to study stable bi-maps $F = (f_1, f_2)$ defined on a smooth closed orientable surface $M \subset \mathbb{R}^3$. Stable bi-maps means a pair of stable maps, i.e., $f_1 : M \to \mathbb{R}$ and $f_2 : M \to \mathbb{R}^2$ are stable maps. Stable maps have been investigated by several authors and have many interesting applications (see, for instance, [3, 4, 8, 11, 13, 18]).

Let us describe the stable bi-maps as above and to show how to associate the graph theory to investigate it.

Denote by $C^\infty(M, \mathbb{R}^p)$ the set of all C^∞ maps from M to $\mathbb{R}^p$, $p = 1, 2$.

Firstly, consider a stable map $f_1 : M \to \mathbb{R}$. For this type of map, it is known that the Reeb graph is a global topological invariant associated to f_1 (cf. [5, 15]). The Reeb graph describes the topology of the surface M. Reeb graphs appear with many applications in Computational Geometry, Computer Graphics, Engineering, Applied Mathematics, etc. We will denote the Reeb graph associated to a stable map $f_1 : M \to \mathbb{R}$ by $\mathscr{R}$-graph of f_1. The Figure 1 shows a practical application of $\mathscr{R}$-graphs on the study of human body shape and posture using 3D images (cf. [17]).

Notice that in Figure 1 (4), we have two distinct body shapes represented by the same $\mathscr{R}$-graph, (c) and (f). Since $\mathscr{R}$-graphs do not distinguish these two body shapes, this kind of problem motivates us to introduce a new graph which encodes information that just the $\mathscr{R}$-graph does not encode.

This new invariant is constructed as follows. We consider a stable map of type $f_2 : M \to \mathbb{R}^2$. From Whitney theorem (cf. [18]), the singular set of f_2 (denoted by $\Sigma f_2 \subset M$) consists of curves of double points, possibly containing isolated cusp points. The apparent contour of f_2 (i.e., $f_2(\Sigma f_2)$ the image of the singular set) consists of a number of immersed curves in $\mathbb{R}^2$ (possibly with cusps) whose self-intersections are all transverse and disjoint from the cusps (if any). The singular and regular components in M codify relevant information about the stable map f_2. In fact, in [8] graphs with weights on the vertices were introduced as a global topological invariant for stable maps of type $f_2 : M \to \mathbb{R}^2$. These weighted graphs describe the position of the singular and the regular sets of f_2 in M. Its edges, vertices and weights corresponding to the singular components, regular components and the genus of the regular components of M, respectively. We will denote the weighted graph associated to $f_2 : M \to \mathbb{R}^2$ by $\mathscr{M}$-graph of f_2.

In Figure 1, if we consider f_2 as the projection map of the human body shapes (4-a) and (4-d) on the (floor) plane, then the $\mathscr{M}$-graphs associated to f_2 can be used to distinguish them while the $\mathscr{R}$-graphs cannot. To illustrate how the $\mathscr{M}$-graphs associated to f_2 can distinguish different body shapes, see Figure 2.

By the other hand, there are situations in the converse sense: we can have the same $\mathscr{M}$-graphs but the $\mathscr{R}$-graphs are different. See, for instance, the Figure 3, (a) and (b).

Then, it seems natural to consider the pair $\mathscr{R}$-graph and $\mathscr{M}$-graph, instead of considering just one of them. The pair captures more information about the topological structure of M than only one of them.
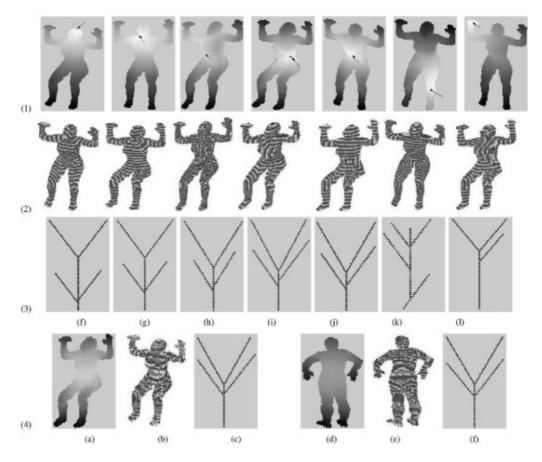
Figure 1: $\mathscr{R}$-graphs associated to human body shapes (for details, see [17]). This figure was extracted from the reference [17], Fig. 2, page 157.
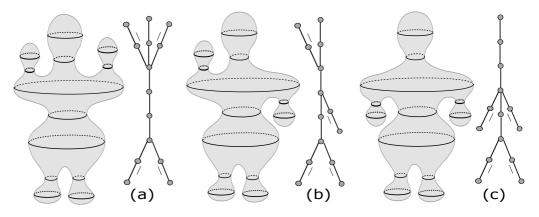

Figure 2: $\mathscr{M}$-graphs related to three distinct human body shapes.

In this way, the motivation of this work is to consider stable bi-maps of type $F = (f_1, f_2)$: $M \to \mathbb{R} \times \mathbb{R}^2$ and its associated $\mathscr{R}\mathscr{M}$-graphs. The $\mathscr{R}\mathscr{M}$-graph is exactly the pair formed by the $\mathscr{R}$-graph associated to f_1 and by the $\mathscr{M}$-graph associated to f_2. Moreover, we can use the $\mathscr{R}\mathscr{M}$-graphs to investigate the topological structure of the surface M and of the singular set Σf_2. Previously, we showed a possible application of $\mathscr{R}\mathscr{M}$-graphs to study patterns of the human body. This kind of application is very interesting to Computer Vision. There will certainly be many other practical applications of such $\mathscr{R}\mathscr{M}$-graphs.

The last part of this paper is dedicated to investigate the graph realization problem. This is a very interesting and difficult problem. Given a graph Γ, in which conditions Γ can be realized as an $\mathscr{R}\mathscr{M}$-graph associated to some bi-stable map $F = (f_1, f_2) : M \to \mathbb{R} \times \mathbb{R}^2$? We answer this question in Section 5 for some cases (see Theorems 5.3, 5.4 and 5.5). Recently, many authors have dedicated themselves to the realization problem of $\mathscr{R}$-graphs associated with Morse functions or Morse-Bott functions (see, for instance, the works of L.P. Michalak [12], I. Gelbukh [6], N. Kitazawa [9], among others). The second and third named authors of this paper, have also a recent work about the realization problem of the calls MB-Reeb graphs [2]. The MB-Reeb graphs are a kind of generalization of the $\mathscr{R}$-graphs and they were introduced in [2] to investigate the topological classification of circle-valued Morse-Bott functions defined on surfaces.

Some techniques applied here for a $\mathscr{M}$-graph such as surgeries, codimension one transitions, etc., are based on the references [8, 13].

2 STABLE BI-MAPS

Let M be a closed orientable surface and $N = \mathbb{R}^p$ ($p = 1, 2$). Two smooth maps $f, g : M \to N$ are said to be $\mathscr{A}$-*equivalent* (or just *equivalent*) if there are orientation-preserving diffeomorphisms, $k : M \to M$ and $l : N \to N$ such that $g \circ k = l \circ f$. A smooth map $f : M \to N$ is said to be *stable* if all maps sufficiently closed to f (with respect to Whitney C^∞-topology) are equivalent to f (see [7] for more details).

A smooth map $F = (f_1, f_2) : M \to \mathbb{R} \times \mathbb{R}^2$ is said to be a *stable bi-map* if each f_i, $i = 1, 2$, is a stable map.

Considering $F = (f_1, f_2) : M \to \mathbb{R} \times \mathbb{R}^2$ be a stable bi-map notice that we have the following properties:

a) Since $f_1 : M \to \mathbb{R}$ is stable then f_1 is Morse with distinct critical values. That is, every critical point of f_1 is non-degenerate and each critical level curve of f_1 has a finite number of critical points, all distincts.

b) Since $f_2 : M \to \mathbb{R}^2$ is stable then its singular points are only folds and isolated cups. Remind that a point $p \in M$ is a regular point of f_2 if the map f_2 is a local diffeomorphism around p. Otherwise, the point p is said to be a singular point. According to Whitney theorem (cf. [18]), the singularities of any stable map $f_2 : M \longrightarrow \mathbb{R}^2$ are (locally) of fold type $(x, y) \mapsto (x, y^2)$ or of cusp type $(x, y) \mapsto (x^3 + yx, y)$.

c) The set of all singular points of f_2, denoted by Σf_2, is called *singular set* of f_2. The singular set of f_2 consists of (finitely many) disjoint embedded closed curves in M. The image of singular set of f_2, i.e., $f_2(\Sigma f_2)$, is called the *apparent contour* of f_2. The apparent contour of f_2 is a finite number of immersed closed plane curves with finite number of cups and finite number of transverse intersections and self-intersections (disjoint from the set of cups). The *regular set* of f_2, given by $M \setminus \Sigma f_2$, consists of all regular points of f_2. Since M is a smooth closed orientable surface, the singular set Σf_2 is a finite collection of closed regular simple curves on M formed by fold points with possible isolated cusp points that divide M in a set of regular regions.

Let $j : M \to \mathbb{R}^3$ be an immersion of M in $\mathbb{R}^3$ and $\vec{v} \neq 0$ be any vector in $\mathbb{R}^3$. We can decompose $\mathbb{R}^3$ in a direct sum $R_v \oplus \mathscr{P}_v$, where R_v is a parallel line to $\vec{v}$ and $\mathscr{P}_v$ is a orthogonal plane to $\vec{v}$. Then we can consider two stable projections as following:

1. $\pi_v^1 : j(M) \to R_v$ given by the restriction to $j(M)$ of the canonical projection of $\mathbb{R}^3$ in R_v.

2. $\pi_v^2 : j(M) \to \mathscr{P}_v$ given by the restriction to $j(M)$ of the canonical projection of $\mathbb{R}^3$ in $\mathscr{P}_v$.

Let $h : R_v \to \mathbb{R}$ and $g : \mathscr{P}_v \to \mathbb{R}^2$ be diffeomorphisms and consider $f_1 : M \to \mathbb{R}$ and $f_2 : M \to \mathbb{R}^2$ two stable maps. Then we can define the following stable maps using π_v^1 and π_v^2:

$$f_1 = h \circ \pi_v^1 \circ j \;\; and \;\; f_2 = g \circ \pi_v^2 \circ j.$$

These stable maps f_1 and f_2 as above defined are called *projection to a parallel line to $\vec{v}$* and *projection to an orthogonal plane to $\vec{v}$*, respectively, associated to the immersion j (see Figure 3).

Observe that when f_1 is a projection to a parallel line to $\vec{v}$ and f_2 is a projection to a orthogonal plane to $\vec{v}$, then the pair $F = (f_1, f_2)$ is clearly a stable bi-map.

From now one, we will always consider in this paper stable bi-maps $F = (f_1, f_2)$ where f_1 is a projection to a parallel line $\vec{v}$, f_2 is a projection to an orthogonal plane to $\vec{v}$ and $\vec{v} \neq 0$ is a fixed vector in $\mathbb{R}^3$.
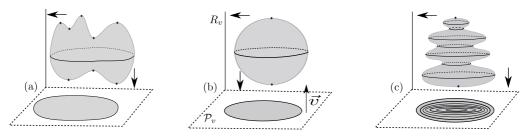

Figure 3: Example of stable bi-maps from sphere.

The Figure 3 illustrates three different stable bi-maps from sphere $\mathbb{S}^2$. Notice that in (a) and (b), the projections to the orthogonal plane $\mathscr{P}_v$ have the same number of connected components of the singular set, while the projections to R_v have distinct number of singular points. Already in (b) and (c), the projections to R_v have the same number of singular points while the projections to $\mathscr{P}_v$ have distint numbers of singular curves. In this way, the classsical invariant related to stable projections to the orthogonal plane $\mathscr{P}_v$ do not distinguish (a) and (b) but they distinguish (b) and (c). By other hand, the classical invariant associated to the projections to the parallel line R_v can distinguish (a) and (b) but not (b) and (c).

In fact, the classical invariant associated to the projection to R_v (i.e., the stable map f_1) was codified in the literature by the Reeb graph associated to f_1. The Reeb graphs were introduced by Reeb in [15]. Here the Reeb graphs will be denoted by $\mathscr{R}$-graphs. The next Subsection 3.1 will be dedicated to explain the $\mathscr{R}$-graphs.

By other hand, the classical invariant associated to the projection to $\mathscr{P}_v$ (i.e., the stable map f_2) was codified in the literature by Hacon-Mendes-Romero in [8], by a graph with weights in the vertices. Here these graphs will be denoted by $\mathscr{M}$-graphs or *Mendes*-graphs. The next Subsection 3.2 will be dedicated to explain the $\mathscr{M}$-graphs.

Figure 4: $\mathscr{R}$-graphs and $\mathscr{M}$-graphs corresponding to the Figure 3.

The Figure 4 illustrates the respectives $\mathscr{R}$-graphs and $\mathscr{M}$-graphs in the three previous examples given in Figure 3. Notice that in (a) and (b) the respective $\mathscr{R}$-graphs are not isomorphic while in (b) and (c) only the $\mathscr{M}$-graphs are not isomorphic. The Figure 5 shows one more example of two stable maps from sphere $\mathbb{S}^2$ and their respective $\mathscr{R}$-graphs and $\mathscr{M}$-graphs.
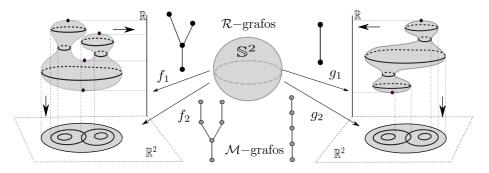

Figure 5: Examples of $\mathscr{R}$-graphs and $\mathscr{M}$-graphs associated to stable maps on sphere.

This suggests that these two graphs togheter may give more information to differ two immersions of M in $\mathbb{R}^3$ that just one of them. This is our motivation to introduce, in the next Section, the called $\mathscr{RM}$-graph which is a pair of graphs.

3 $\mathscr{RM}$-GRAPHS ASSOCIATED TO BI-STABLE MAPS

Given a smooth closed orientable surface M, let $j : M \to \mathbb{R}^3$ be an embedding and as said before, let us consider bi-stable maps of type $F = (f_1, f_2) : M \to \mathbb{R} \times \mathbb{R}^2$, where f_1 is a projection in a line and f_2 is a projection on a plane. By simplicity, if we consider $R_v = \mathbb{R}$ and $\mathscr{P}_v = \mathbb{R}^2$, we can take

$$f_1 = \pi_1 \circ j \ \text{ and } \ f_2 = \pi_2 \circ j,$$

where π_i denotes the canonical projection in $\mathbb{R}^i$, $i = 1, 2$.

Definition 3.1. If $\mathscr{G}^1$ is the $\mathscr{R}$-graph associated to $f_1 : M \to \mathbb{R}$ and $\mathscr{G}^2$ is the $\mathscr{M}$-graph associated to $f_2 : M \to \mathbb{R}^2$, then we say that the pair of graphs $(\mathscr{G}^1, \mathscr{G}^2)$ is the $\mathscr{RM}$-*graph* associated to the stable bi-map $F = (f_1, f_2) : M \to \mathbb{R} \times \mathbb{R}^2$.

In the next pictures, the $\mathscr{RM}$-graphs will be illustrated always in this order $(\mathscr{G}^1, \mathscr{G}^2)$. Moreover, the notation $\mathscr{G}^i(V^i, E^i)$ will indicate that the graph $\mathscr{G}^i$ is a graph with V^i vertices and E^i edges, $i = 1, 2$.

In an $\mathscr{RM}$-graph, the $\mathscr{R}$-graph contributes to determine the position of the maximum and minimum points (local and global) of f_1 while the $\mathscr{M}$-graph contributes to determine the position of the regular regions and singular curves of f_2 in M.

3.1 $\mathscr{R}$-graphs

Given a stable map $f_1 : M \to \mathbb{R}$ we consider the following equivalence relation on M:

$x \sim y \Leftrightarrow f_1(x) = f_1(y)$ and x and y are in the same connected component of $f_1^{-1}(f_1(x))$.

Then the quotient space $M/\sim$ admits the structure of a connected graph where the vertices are the connected components of critical level curves $f_1^{-1}(v)$ which contains critical points of f_1 and each edge is formed by points that correspond to connected components of level curves $f_1^{-1}(w)$, where $w \in \mathbb{R}$ is a regular value and $v \in \mathbb{R}$ is a critical value of f_1.

Each vertex of the graph can be of three types, depending on the critical points in the connected component as shown in Figure 6.
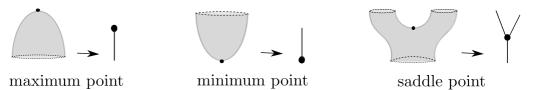

Figure 6: Incidence rules for the vertices in a Reeb graph.

Let $v_1, \ldots, v_r \in \mathbb{R}$ be the critical values of f_1. We choose a base point $v_0 \in \mathbb{R}$ and an orientation. We can reorder the critical values such that $v_0 \leq v_1 < \cdots < v_r$ and we label each vertex with the index $i \in \{1, \ldots, r\}$, if it corresponds to the critical value v_i.

Definition 3.2. The graph given by $M/\sim$ together with the labels of the vertices, as previously defined, is said to be the *Reeb graph* (or $\mathscr{R}$*-graph*) associated to $f_1 : M \to \mathbb{R}$.
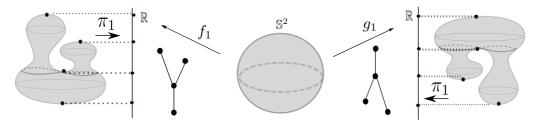

Figure 7: Examples of $\mathscr{R}$-graphs from sphere.

It is known that the Reeb graph is a complete topological invariant for stable functions (cf. [1]). The example in Figure 7 shows that the $\mathscr{R}$-graph is an invariant that distinguishes what the image set of the critical points cannot tell us.

Follows from the possible incidence rules of edges and vertices in an $\mathscr{R}$-graph that all its vertices have degree 1 or 3. Graphs with this property will be called here *1-trivalent graphs*.

Hence, the $\mathscr{R}$-graph associated to a stable map f_1 is 1-trivalent. Moreover, the Euler characteristic of M is given by $\chi(M) = 2(V^1 - E^1)$. In other words, the topology of surface M can be determined by the $\mathscr{R}$-graph associated to f_1.

Follows from the Poincaré-Hopf theorem that every $\mathscr{R}$-graph associated to a stable map $f_1 : \mathbb{S}^2 \to \mathbb{R}$ is a 1-trivalent tree.

Theorem 3.1. *Any 1-trivalent graph* $\mathscr{G}^1(V^1, E^1)$ *is a* $\mathscr{R}$*-graph associated to a stable map* $f_1 : M \to \mathbb{R}$ *where the Euler characteristic of M is* $\chi(M) = 2(V^1 - E^1)$.

Proof. Given a 1-trivalent graph $\mathscr{G}^1(V^1, E^1)$, we can construct a surface M such that $\mathscr{G}^1(V^1, E^1)$ is the $\mathscr{R}$-graph associated to the height function $f : M \to \mathbb{R}$. In fact, consider an embedding of the graph $\mathscr{G}^1(V^1, E^1)$ in $\mathbb{R}^3$. Let M be the boundary of a thin tubular neighborhood of $\mathscr{G}^1(V^1, E^1)$. Then M is diffeomorphic to a surface with $\chi(M) = 2(V^1 - E^1)$. Moreover, the restriction of the height function on M, $f : M \to \mathbb{R}$, is a stable map whose $\mathscr{R}$-graph is equivalent to $\mathscr{G}^1(V^1, E^1)$. $\square$

3.2 $\mathscr{M}$-graphs

Given a stable map $f_2 : M \to \mathbb{R}^2$, its topological information may be conveniently encoded in a determined weighted graph. In fact, given the pair $(M, \Sigma f_2)$, we may reconstruct (up to diffeomorphism) a weighted graph associated to f_2 (cf. [8]), in the following sense: the edges and vertices of this weighted graph correspond to the singular curves and the connected components

of the regular set, respectively. An edge is incident to a vertex if and only if the corresponding singular curve to the edge lies in the boundary of the regular region corresponding to the vertex. The weight of a vertex is defined as the genus of the corresponding region. This graph is called $\mathscr{M}$-*graph* (or *Mendes*-graph) associated to f_2.

It is known that the $\mathscr{M}$-graph is a complete topological invariant for stable maps from M to the plane (cf. [8]).

Let $\mathscr{G}^2(V^2, E^2, W^2)$ be the $\mathscr{M}$-graph associated to f_2, where V^2, E^2 and W^2 correspond to the number of vertices, edges and the total weight of the graph, respectively. Then E^2 represents the number of connected components of Σf_2; V^2 the number of connected components of $M \setminus \Sigma f_2$ and W the total sum of genus of the components of $M \setminus \Sigma f_2$.

If $W^2 = 0$, that is, if $\mathscr{G}^2$ is a graph without weight, we will denote by simplicity $\mathscr{G}^2(V^2, E^2)$ omitting W^2 in the graph notation.
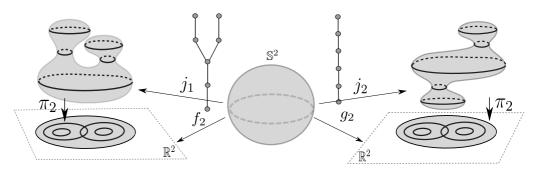

Figure 8: Examples of $\mathscr{M}$-graphs associated to stable maps from sphere.

The Figure 8 illustrates two stable maps $f_2, g_2 : \mathbb{S}^2 \to \mathbb{R}^2$ whose $\mathscr{M}$-graphs are non equivalent, where j_i indicates the respective embedding from $\mathbb{S}^2$ in $\mathbb{R}^3$ and π_i the canonical projection, $i = 1, 2$. This example shows that the $\mathscr{M}$-graph is an invariant that distinguishes what the apparent contour sets of f_2 and g_2 can not distinguish.

Given a stable map $f_2 : M \to \mathbb{R}^2$ always it is possible to obtain its $\mathscr{M}$-graph associated. Moreover, the Euler characteristic of M is given by $\chi(M) = 2(V^2 - E^2 - W^2)$. In other words, the topology of surface M can be determined by $\mathscr{M}$-graph $\mathscr{G}^2(V^2, E^2, W^2)$ associated to f_2.

Given the orientations of M and $\mathbb{R}^2$, a region of M is said to be *positive* (resp. *negative*) if the map f_2 preserves (resp. reverses) orientation. Since each component of Σf_2 is the boundary of a positive and a negative region, the signs of the vertices are assigned alternately, that is, the $\mathscr{M}$-graph associated to stable map $f_2 : M \to \mathbb{R}^2$ is *bipartite*.

To be a bipartite graph is a necessary condition for a graph to be a $\mathscr{M}$-graph for some stable map $f_2 : M \to \mathbb{R}^2$.

Theorem 3.2. ([8]) *Any bipartite connected graph (with arbitrarily weighted vertices) is the $\mathscr{M}$-graph of a stable map $f_2 : M \to \mathbb{R}^2$.*

The proof of Theorem 3.2 is based in a convenient manipulation of codimension one transitions (lips and beaks) in the space $C^\infty(M, \mathbb{R}^2)$ and convenient surgeries of stable maps (see [8] for more details). Transitions and surgeries involving stable maps will be treated with more details in the next Section.

As a consequence of Theorem 3.2, any tree with $W^2 = 0$ may be realized as the $\mathscr{M}$-graph of some stable map $f_2 : \mathbb{S}^2 \to \mathbb{R}^2$.

From now on, we focus on $\mathscr{M}$-graphs without weighted vertices (that is, $W^2 = 0$). The case $W^2 > 0$ will be studied in a future work in progress.

4   TOOLS USED TO CONSTRUCT STABLE BI-MAPS

Let $\mathscr{E}^\infty(M, \mathbb{R}^p)$ be the set of all stable maps in $C^\infty(M, \mathbb{R}^p)$, $p = 1, 2$.

In this work we are considering stable bi-maps of type $F = (f_1, f_2) : M \to \mathbb{R} \times \mathbb{R}^2$ which can be decomposed (locally) as $f_i = \pi_i \circ j$, $i = 1, 2$, where j is an embedding from M in $\mathbb{R}^3$ and π_i are the canonical projections from $j(M)$ to $\mathbb{R}$ and $\mathbb{R}^2$, respectively, $i = 1, 2$. Replacing the embedding j by another embedding from M in $\mathbb{R}^3$, we can obtain new stable bi-maps. This procedure can be done by taking small perturbations of the embedding j, so that they may alter or not the images of the projections π_1 and π_2. The new stable bi-maps obtained in this procedure have associated new $\mathscr{R}\mathscr{M}$-graphs. Then, it is natural to ask whether these changes modify the new $\mathscr{R}\mathscr{M}$-graphs or not.

The alterations used here to obtain new stable bi-maps correspond to transitions and surgeries and they are described with more details in the next Subsections.

4.1   Elementary Morse transitions

In this Subsection let us consider stable maps in $\mathscr{E}^\infty(M, \mathbb{R})$.

A Morse transition corresponds to an isotopy from a given stable map to another in a different path component of $\mathscr{E}^\infty(M, \mathbb{R})$. Thus, a Morse transition allows to transform a stable map $f_1 : M \to \mathbb{R}$ in another $\tilde{f}_1 : M \to \mathbb{R}$ in such a way that their respective $\mathscr{R}$-graphs have a different number of vertices or the same number of vertices with noncompatible labels.

A Morse transition T is called *elementary* if the isotopy T transforms f_1 in $\tilde{f}_1$ through one of the following ways:

[C] The isotopy T creates a new edge in $\mathscr{R}$-graph of f_1. That is, if $T(0) = f_1$ and its $\mathscr{R}$-graph has s saddles and m max/min points then $T(1) = \tilde{f}_1$ and the $\mathscr{R}$-graph of $\tilde{f}_1$ has $s + 1$ saddles and $m + 1$ max/min points, with the new saddle and max/min point being connected by a new edge.

[$-\mathbf{C}$] It is the inverse transition of **C**. That is, when the isotopy collapses an edge of $\mathscr{R}$-graph of f_1, with the vertices that were removed being previously connected by an edge. In this case, the $\mathscr{R}$-graph of $\tilde{f}_1$ has $s-1$ saddles and $m-1$ max/min points.

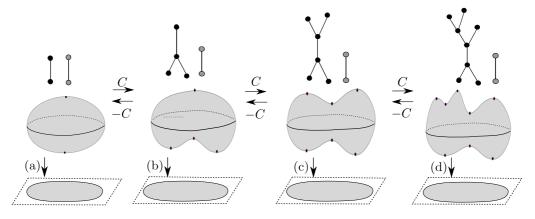The Figure 9 indicates examples of elementary Morse transitions.

Figure 9: The effect of the elementary Morse transitions in the $\mathscr{R}$-graphs.

For more details about the consequences of Morse transitions in a Reeb graph see [10].

Since elementary Morse transitions do not generate any new critical curve related to projection π_2 (in the plane), the $\mathscr{M}$-graph has no change after **C** or $-\mathbf{C}$ transitions. In other words, elementary Morse transitions alter the $\mathscr{R}\mathscr{M}$-graph associated to original stable bi-map $F = (f_1, f_2) = (\pi_1 \circ j, \pi_2 \circ j)$, changing only its $\mathscr{R}$-graph.

Definition 4.3. *Given a $\mathscr{R}$-graph $\mathscr{G}^1$, we say that a **C** transition is a* 1-extension *over the graph $\mathscr{G}^1$.*

A sequence of n 1-extensions over a $\mathscr{R}$-graph increases n vertices of degree 1 (max/min points) and n vertices of degree 3 (saddles) over the original $\mathscr{R}$-graph.

Any 1-trivalent tree $\mathscr{G}^1(V^1, V^1 - 1)$ can be obtained as a $\mathscr{R}$-graph of a stable map from M to $\mathbb{R}$ by applying a sequence with $(V^1 - 2)/2$ 1-extensions over the $\mathscr{R}$-graph of canonical height function from $\mathbb{S}^2$ to $\mathbb{R}$.

Proposition 4.1. *All pair of trees $(\mathscr{G}^1(V^1, V^1 - 1), \mathscr{G}^2(2, 1))$ is a $\mathscr{R}\mathscr{M}$-graph of some stable bi-map $F = (f_1, f_2) : \mathbb{S}^2 \to \mathbb{R} \times \mathbb{R}^2$, where $\mathscr{G}^1(V^1, V^1 - 1)$ is a 1-trivalent tree.*

Proof. Since $\mathscr{G}^1(V^1, V^1 - 1)$ is an 1-trivalent tree, then V^1 is even and $(V^1 - 2)/2$ is a integer number. Consider the standard stable bi-map $G = (g_1, g_2) : \mathbb{S}^2 \to \mathbb{R} \times \mathbb{R}^2$ where $g_i = \pi_i \circ j$ and $j : \mathbb{S}^2 \to \mathbb{R}^3$ is the inclusion.

Let $(\mathscr{G}^1(2, 1), \mathscr{G}^2(2, 1))$ be the $\mathscr{R}\mathscr{M}$-graph associated to G. After a sequence with $(V^1 - 2)/2$ 1-extensions over the $\mathscr{R}\mathscr{M}$-graph of G without altering the singular set of g_2, we obtain a new

stable bi-map $F = (f_1, f_2) : \mathbb{S}^2 \to \mathbb{R} \times \mathbb{R}^2$ which realizes the graph $(\mathscr{G}^1(V^1, V^1 - 1), \mathscr{G}^2(2, 1))$. In fact, each 1-extension increases two edges and two vertices in the $\mathscr{R}$-graph and do not alter the $\mathscr{M}$-graph. □

4.2   Lips, beaks and swallowtail transitions

In this Subsection we will consider transitions that alter only the $\mathscr{M}$-graph in a $\mathscr{R}\mathscr{M}$-graph associated to a stable bi-map $F = (f_1, f_2) : M \to \mathbb{R} \times \mathbb{R}^2$. They are the same transitions that change the regular and singular sets of f_2, namely the *lips transitions*, denoted by **L** and *beaks transitions*, denoted by **B** (see Figure 10). We denote by $-\mathbf{B}$ and $-\mathbf{L}$, respectively, the inverse transitions of **B** and **L**. These transitions also change the number of cusps by ± 2 and they are sufficient to show that any tree with weight equal zero can be realized as a graph of a stable map from $\mathbb{S}^2$ to $\mathbb{R}^2$ (see [8]).
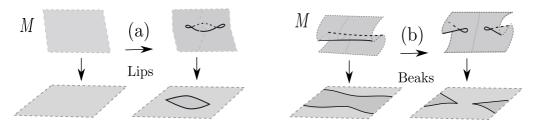

Figure 10: Lips and beaks transitions.

Let $G^2(V^2, E^2)$ be the $\mathscr{M}$-graph (without weight) associated to a stable map $f_2 : M \to \mathbb{R}^2$. Then, the lips transition increases by 1 the number of regions in M (i.e., vertices in V^2) and the number of singular curves in M (i.e., edges in E^2). The beaks transition can be classified in four different cases (see Figure 12):
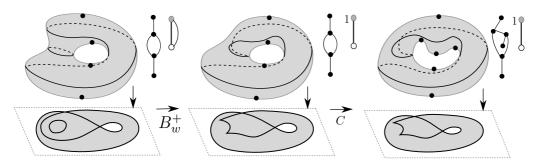

Figure 11: Beaks transition and *C*-transition on the torus.

$\mathbf{B}_v^+$: beaks transition increases by 1 the number of regular regions, i.e., it adds 1 vertex and 1 edge on the $\mathscr{M}$-graph;

$\mathbf{B}_v^-$: beaks transition decreases by 1 the number of regular regions, therefore it removes 1 vertex and 1 edge on the $\mathcal{M}$-graph (see Figure 13);

$\mathbf{B}_w^+$: beaks transition increases by 1 the weight, maintains the number of regular regions (vertices) but decreases by 1 the number of edges (see Figure 11);

$\mathbf{B}_w^-$: beaks transition decreases by 1 the weight, maintains the number of regular regions (vertices) but increases by 1 the number of edges.
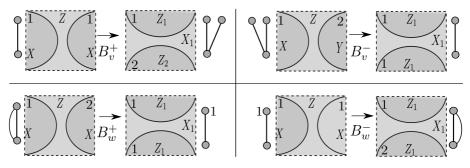

Figure 12: Decomposition of beaks transition.

The four types of beaks transition are illustrated (locally) in Figure 12, where in the picture X, X_1, Y, Z, Z_1 and Z_2 denote (locally) the regular regions where the transitions hold and the numbers 1 and 2 represent the number of singular curves.

Definition 4.4. Given a $\mathcal{M}$-graph $G^2(V^2, E^2)$ (without weight), we say that a composition of a lips transition with a beaks transition (in this order) is a *2-extension* over a $\mathcal{M}$-graph when:

1. a lips transition $\mathbf{L}$ creates a singular curve α with 2 cusps and 1 new regular region D;

2. a beaks transition $-\mathbf{B}_v^-$ eliminates the 2 cusps, dividing α into two new singular curves and border of the new region D', as illustrate Figure 13.
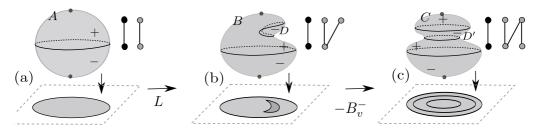

Figure 13: Lips and beaks transitions and 2-extensions.

The lips transition creates a new region D inside of region A, decomponding A into B and D, where B is homeomorphic to a cilinder and D is homeomorphic to a disk. The beaks transition

transformes the regions B and D into C and D', where D' is homeomorphic to a cilinder and C is homeomorphic to a disk.

Lips and beaks transitions can modify the singular set of a stable map from M to the plane, and do not alter the singular set of the height function. That is, the $\mathscr{R}$-graphs are preserved by 2-extensions while the $\mathscr{M}$-graphs always add two vertices (linked by one edge) with degree two on the graph. The Figure 13 illustrates a sequence of transitions that alter the $\mathscr{M}$-graph but they do not the $\mathscr{R}$-graph.

Definition 4.5. We call *line graph*, and denoted it by $\mathscr{L}^2(k)$, a graph with k vertices with degree 2 and $k-1$ edges.

In the Figure 13 we have three examples of $\mathscr{M}$-graphs which are line graphs: (a) $\mathscr{L}^2(2)$; (b) $\mathscr{L}^2(3)$ and (c) $\mathscr{L}^2(4)$. Moreover, the lips transition **L** holds in a positive region of $\mathbb{S}^2$ creating a new singular curve with 2 cusps (see (b)). The beaks transition $-\mathbf{B}_v^-$ in the negative new region eliminates 2 cusps and adding a new singular curve (see (c)).

Applying 2-extensions we can show that all line graph $\mathscr{L}^2(k)$ is a $\mathscr{M}$-graph of some stable map $f_2 : \mathbb{S}^2 \to \mathbb{R}^2$. This is a consequence of Theorem 3.2.

4.3   Surgeries of stable bi-maps

Are considered two types of surgeries of stable bi-maps: horizontal and vertical surgeries. We are interested to know the effects of these surgeries over the $\mathscr{R}\mathscr{M}$-graphs. This study is based in the concepts introduced in [8].

Let $F = (f_1, f_2) : M \to \mathbb{R} \times \mathbb{R}^2$ be a bi-stable map, P and Q be two any regions of surface M, where M may or may not be connected.

Horizontal surgery $\mathscr{S}^h$: Let $p \in P, q \in Q$ be two singular points of f_2. A *bridge* is an embedded arc β in $\mathbb{R}^2$, which connects the set of singular values of f_2 (or apparent contour) in its two end points (and nowhere else). A new stable map f_{2h} can be constructed as follows: the bridge links the apparent contour of f_2 in its points, $f_2(p)$ and $f_2(q)$. Choose small disks D_p, D_q in M centered at $p, q \in \Sigma f_2$, respectively. We can choose small enough disks such that they do not contain any critical point of f_1. Replace the interiors of D_p and D_q by a tube (i.e., an annulus) connecting these two small disks obtaining a new connected surface N. Then f_1 and f_2 may be extended over the tube to give new stable maps f_{1h} and f_{2h}, in such way that f_1 has only 2 saddle points in this tube, as shown (locally) in Figure 14.

The horizontal surgery $\mathscr{S}^h$ connects the two regular regions of f_1 and adds 2 saddle points, while in f_2 the horizontal surgery $\mathscr{S}^h$ effects are:

   i) it links the 2 singular curves if p and q are in two disjoint singular curves (see the graphs in Figure 16 (a)-(b));
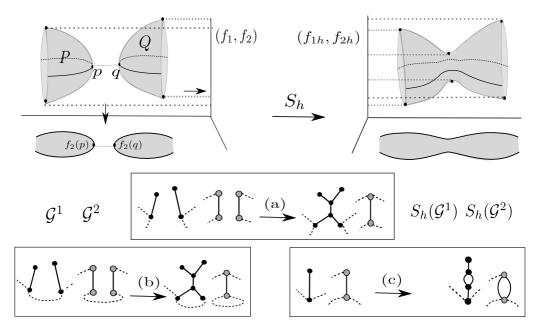
Figure 14: Horizontal surgery example.

ii) it separates a singular curve into two curves, if p and q are in the same singular curve (see the graphs in Figure 16 (c)).

Vertical surgery $\mathscr{S}^v$: Let $p \in P, q \in Q$ be two singular points of f_2. We take a surgery between P e Q by identifying two small topological disks D_p and D_q, one positive and one negative, such that each one of them contains only 1 critical point of f_1 in their interior being 1 maximum and 1 minimum, and its boundary is a connected component of a regular level curve of f_1. The disks are replaced by a tube which is mapped into $\mathbb{R}$, with no singular points in the interior of the tube. The stable map f_1 may be extended over the tube to a new stable map f_{1v} from a new connected surface N to $\mathbb{R}$. Also, the stable map f_2 can be extended to a new stable map $f_{2v} : N \to \mathbb{R}^2$ with one fold curve in the tube (see Figure 15).

The vertical surgery $\mathscr{S}^v$ identifies a neighborhood of a maximum point of f_1 as a neighborhood of a minimum point of f_1, eliminating two singular points. In f_2, the surgery $\mathscr{S}^v$ always creates a new singular curve. In other words, the vertical surgery $\mathscr{S}^v$ takes away two critical points of the singular set Σf_1 while it adds one critical curve to Σf_2 (see Figure 15 and 16-(b)).

Notice that the regions P and Q can be in a same connected component of M or in two different connected components. If P and Q are regions of the same connected component of M the singular points $p, q \in \Sigma f_2$ may or may not be in the same singular curve.

We denote by $\mathscr{S}^h(f_1, f_2) = (f_{1h}, f_{2h}) : N \to \mathbb{R} \times \mathbb{R}^2$ the new stable bi-map resulting after the horizontal surgery $\mathscr{S}^h$, and by $\mathscr{S}^h(\mathscr{G})$ the effect in the graph $\mathscr{G}$ after applying a horizontal surgery $\mathscr{S}^h$. Analogously we denote by $\mathscr{S}^v(f_1, f_2) = (f_{1v}, f_{2v}) : N \to \mathbb{R} \times \mathbb{R}^2$ the new stable
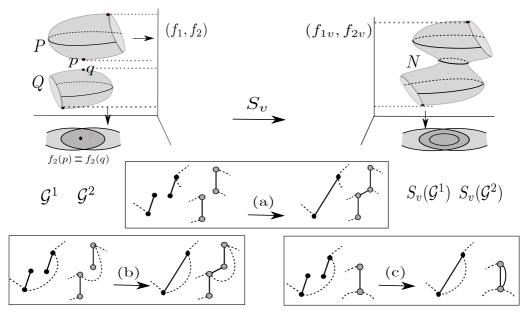
Figure 15: Vertical surgery of bistable maps.

bi-map resulting after the vertical surgery $\mathscr{S}^v$ and by $\mathscr{S}^v(\mathscr{G})$ the effect in the graph $\mathscr{G}$ after applying a vertical surgery $\mathscr{S}^v$.

Let P and Q be two regions of M that are in two connected component of M, then the surgeries $\mathscr{S}^h$ and $\mathscr{S}^v$ over P and Q are called *connected horizontal sum* (see Figure 15-(a)) and *connected vertical sum* (see Figure 15-(a)).

Definition 4.6. We denote by $\mathscr{S}^{h1}$ (resp. $\mathscr{S}^{v1}$) the horizontal surgery (resp. vertical surgery) of stable maps from M to the plane that connects two regions of a connected surface M. We denote by $\mathscr{S}^{h0}$ (resp. $\mathscr{S}^{v0}$) the horizontal surgery (resp. vertical surgery) that connects two regular regions of two different connected components of M.

This local process of f_2, for $\mathscr{S}^{\eta\alpha}$ ($\eta = h, v$ and $\alpha = 0, 1$) is illustrated in Figures 14 and 15, which shows the effect of these surgeries on the graphs. It induces the following surgeries on the $\mathscr{R}$-graphs and $\mathscr{M}$-graphs (see Figure 15):

A horizontal surgery on graphs which identifies two edges ur and vs, identifying the vertices u with v and r with s, will be denoted by:

(a) $\mathscr{S}^{h0}$: when ru and sv are in different connected graphs, joining these two graphs (Figure 14-(a)).

(b) $\mathscr{S}^{h1}$: when ru and sv are in the same connected component of a graph, creating a new cycle in the graph (see Figure 14-(b) and (c)).

A vertical surgery on graphs which connects two vertices, r positive and v negative, by an edge rv, will be denoted by:

(c) $\mathscr{S}^{v0}$: when r and v are in different connected graphs, joining these two graphs (see Figure 15-(a)).

(d) $\mathscr{S}^{v1}$: when r and v are in the same connected graph, creates a new cycle in the graph (see Figure 15-(b) and (c)).

The next result is a consequence from horizontal surgery and vertical surgeries.

Proposition 4.2. *Let* $(\mathscr{G}_1^1, \mathscr{G}_1^2)$ *and* $(\mathscr{G}_2^1, \mathscr{G}_2^2)$ *be the* $\mathscr{RM}$*-graphs associated to two stable bi-maps* $F = (f_1, f_2) : P \longrightarrow \mathbb{R} \times \mathbb{R}^2$ *and* $G = (g_1, g_2) : Q \longrightarrow \mathbb{R} \times \mathbb{R}^2$, *respectively. Then* $(\mathscr{S}^{\alpha\eta}(\mathscr{G}_1^1, \mathscr{G}_2^1), \mathscr{S}^{\alpha\eta}(\mathscr{G}_1^2, \mathscr{G}_2^2))$ *is the* $\mathscr{RM}$*-graph associated to the stable bi-map*

$$(\mathscr{S}^{\alpha\eta}(f_1, g_1), \mathscr{S}^{\alpha\eta}(f_2, g_2)) : \mathscr{S}^{\alpha\eta}(P, Q) \to \mathbb{R} \times \mathbb{R}^2, \ \alpha = h, v \text{ and } \eta = 0, 1.$$

The Figure 16 illustrates examples of surgeries of stable maps from sphere: (a) horizontal surgery $\mathscr{S}^{h1}$ and (b) vertical surgery $\mathscr{S}^{v1}$.
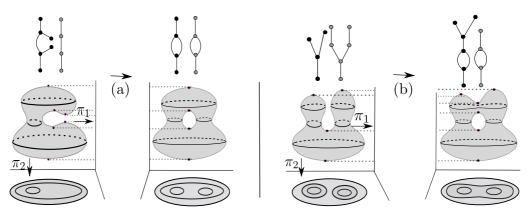

Figure 16: Examples of surgeries: (a) vertical and (b) horizontal.

5 REALIZATION OF GRAPHS $(\mathscr{G}^1, \mathscr{G}^2)$

Lemma 5.1. *All pair of trees* $(\mathscr{G}^1(2, 1), \mathscr{G}^2(V^2, V^2 - 1))$ *is a* $\mathscr{RM}$*-graph of some stable bi-map* $F = (f_1, f_2) : \mathbb{S}^2 \to \mathbb{R} \times \mathbb{R}^2$.

Proof. Consider the pair of canonical maps (given by height function) $G = (g_1, g_2) : \mathbb{S}^2 \to \mathbb{R} \times \mathbb{R}^2$, such that the $\mathscr{RM}$-graph associated to G is $(\mathscr{G}^1(2, 1), \mathscr{G}^2(2, 1))$. Since $\mathscr{G}^2(V^2, V^2 - 1)$ is a tree, let $\mathscr{L}^2(k+1)$ be the biggest line subgraph of $\mathscr{G}^2(V^2, V^2 - 1)$ which connects two peripheral vertices of $\mathscr{G}^2(V^2, V^2 - 1)$, where $k + 1 \leq V^2$. Then, the pair $(\mathscr{G}^1(2, 1), \mathscr{L}^2(k+1))$ can be realized as the following:

i) If k is odd, $k-1$ is even. Passing through a sequence with $(k-1)/2$ of 2-extensions (without altering the singular set of g_1), we obtain a stable bi-map $H = (h_1,h_2): \mathbb{S}^2 \to \mathbb{R} \times \mathbb{R}^2$ which realizes the graph $(\mathscr{G}^1(2,1), \mathscr{L}^2(k+1))$, because each 2-extension increases two edges and two vertices in the $\mathscr{M}$-graph and does not change the $\mathscr{R}$-graph. After this, we can obtain a stable bi-map $F = (f_1,f_2): \mathbb{S}^2 \to \mathbb{R} \times \mathbb{R}^2$, as required, realizing the $\mathscr{RM}$-graph $(\mathscr{G}^1(2,1), \mathscr{G}^2(V^2, V^2-1))$, taking $V^2 - k$ lips transitions over $H = (h_1,h_2)$, in convenient regions.

ii) If k is even, we can first obtain a stable bi-map $H = (h_1,h_2)$ which realizes the graph $(\mathscr{G}^1(2,1), \mathscr{L}^2(k+1))$ as done in item i). Then, we can obtain a stable bi-map $F = (f_1,f_2): \mathbb{S}^2 \to \mathbb{R} \times \mathbb{R}^2$, as required, realizing the $\mathscr{RM}$-graph $(\mathscr{G}^1(2,1), \mathscr{G}^2(V^2, V^2-1)$, taking $V^2 - k + 1$ lips transitions over $H = (h_1,h_2)$, in convenient regions. $\square$

Proposition 5.3. *If $\mathscr{G}^1$ is a 1-trivalent tree and $\mathscr{G}^2$ is a tree whithout weights then the graph $(\mathscr{G}^1, \mathscr{G}^2)$ is a $\mathscr{RM}$-graph of some stable bi-map $F = (f_1,f_2): \mathbb{S}^2 \to \mathbb{R} \times \mathbb{R}^2$.*

Proof. Let $\mathscr{G}^1(V^1, V^1-1)$ be a 1-trivalent tree and $\mathscr{G}^2(V^2, V^2-1)$ be a tree with $W^2 = 0$. Consider $\mathscr{L}^2(k+1)$ the biggest line subgraph of $\mathscr{G}^2(V^2, V^2-1)$. Then by Lemma 5.1, the graph $(\mathscr{G}^1(2,1), \mathscr{L}^2(k+1))$ can be realized by some stable bi-map $G = (g_1,g_2): \mathbb{S}^2 \to \mathbb{R} \times \mathbb{R}^2$. Since V^1 is even and each 1-extension increases 2 vertices and 1 edge to the $\mathscr{R}$-graph, then passing through a sequence with $(V^1-2)/2$ 1-extensions over $G = (g_1,g_2)$ we obtain a stable bi-map $F = (f_1,f_2): \mathbb{S}^2 \to \mathbb{R} \times \mathbb{R}^2$ which realizes the graph $(\mathscr{G}^1(V^1, V^1-1), \mathscr{G}^2(V^2, V^2-1))$, as required. $\square$

From Poincaré-Hopf theorem, Theorem 3.2 and Proposition 5.3, we obtain the following result:

Theorem 5.3. *A graph $(\mathscr{G}^1, \mathscr{G}^2)$ is a $\mathscr{RM}$-graph for a stable bi-map $F = (f_1,f_2): \mathbb{S}^2 \to \mathbb{R} \times \mathbb{R}^2$ if and only if $\mathscr{G}^1$ is a tree 1-trivalent and $\mathscr{G}^2$ is a tree without weights (i.e., with $W^2 = 0$).*

Theorem 5.4. *Let $\mathscr{G}^1$ be a 1-trivalent graph and $\mathscr{G}^2$ be a bipartite graph (with $W^2 = 0$). Suppose $\chi(\mathscr{G}^1) = \chi(\mathscr{G}^2)$. Then the graph $(\mathscr{G}^1, \mathscr{G}^2)$ is a $\mathscr{RM}$-graph associated to a stable bi-map $F = (f_1,f_2): M \to \mathbb{R} \times \mathbb{R}^2$, where $\chi(M) = 2\chi(\mathscr{G}^1) = 2\chi(\mathscr{G}^2)$.*

Proof. Since $\chi(\mathscr{G}^1) = \chi(\mathscr{G}^2)$, both graphs have the same number m of cycles. Consider a pair of support trees $(\mathscr{T}^1, \mathscr{T}^2)$ defined in the following way:

i) $\mathscr{T}^1$ is obtained by choosing one edge in each one of the m cycles of $\mathscr{G}^1$ and subdividing each chosen edge obtaining m new vertices of degree 2. Then we cleave each new vertex v_i $(i = 1, \cdots, m)$ in to two new vertices v_{i1} and v_{i2}, obtaining $2m$ new vertices of degree 1.

ii) $\mathscr{T}^2$ is a spanning tree of $\mathscr{G}^2$, that is, a tree that contains all the vertices of $\mathscr{G}^2$, obtained by removing one edge of each cycle of $\mathscr{G}^2$.

By Theorem 5.3, $(\mathscr{T}^1, \mathscr{T}^2)$ is a $\mathscr{RM}$-graph of a stable bi-map $G = (g_1,g_2): \mathbb{S}^2 \longrightarrow \mathbb{R} \times \mathbb{R}^2$. Consider the regions U_{i1} and U_{i2} of $\mathbb{S}^2$ corresponding to the neighborhoods of the points associated with a pair of vertices v_{i1} and v_{i2} obtained in (i), respectively. For each pair of vertices

v_{i1} and v_{i2}, we may realize a vertical surgery over U_{i1} and U_{i2} obtaining a new stable bi-map $F = (f_1, f_2) : M \longrightarrow \mathbb{R} \times \mathbb{R}^2$ (where M is a surface with genus m) which realizes the $\mathscr{RM}$-graph $(\mathscr{G}^1, \mathscr{G}^2)$. $\qquad\qquad\Box$

The next result is a consequence of the previous results and remarks.

Theorem 5.5. *Consider a pair of graphs* $(\mathscr{G}^1, \mathscr{G}^2)$, *with* $\chi(\mathscr{G}^1) = \chi(\mathscr{G}^2)$. *Then* $(\mathscr{G}^1, \mathscr{G}^2)$ *is a* $\mathscr{RM}$-graph for some stable bi-map $F = (f_1, f_2) : M \longrightarrow \mathbb{R} \times \mathbb{R}^2$, *where M is a closed oriented surface with* $\chi(M) = 2\chi(\mathscr{G}^1) = 2\chi(\mathscr{G}^2)$, *if and only if* $\mathscr{G}^1$ *is a 1-trivalent graph and* $\mathscr{G}^2$ *is a bipartite graph without weights (i.e.* $W^2 = 0$).

Acknowledgments

REFERENCES

[1] V.I. Arnold. Topological classification of Morse functions and generalisations of Hilbert's 16-th problem. *Mathematical Physics, Analysis and Geometry*, **10** (2007), 227–236.

[2] E.B. Batista, J.C.F. Costa & I.S. Meza-Sarmiento. Topological classification of circle-valued simple Morse–Bott functions. *J. Singul*, **17** (2018), 388–402.

[3] E.B. Batista, J.C.F. Costa & J.J. Nuño-Ballesteros. The Reeb graph of a map germ from R^3 to R^2 with isolated zeros. *Proc. Edinb. Math. Soc.*, **60**(2) (2017), 388–402.

[4] E.B. Batista, J.C.F. Costa & J.J. Nuño-Ballesteros. The Reeb graph of a map germ from R^3 to R^2 without isolated zeros. *Bull. Braz. Math. Soc. (N.S.)*, **49** (2018), 369–394.

[5] S. Biasotti, D. Giorgi, M. Spagnuolo & B. Falcidieno. Reeb graphs for shape analysis and applications. *Theoretical computer science*, **392**(1-3) (2008), 5–22.

[6] I. Gelbukh. Realization of a Graph as the Reeb Graph of a Morse–Bott or a Round Function. *Studia Scientiarum Mathematicarum Hungarica*, **59**(1) (2022), 1–16.

[7] M. Golubitsky & V. Guillemin. Stable mappings and their singularities. In "Graduate Texts in Mathematics 14", volume 14. Springer Science & Business Media (2012).

[8] D. Hacon, C.M. de Jesus & M.R. Fuster. Stable maps from surfaces to the plane with prescribed branching data. *Topology and its Applications*, **154**(1) (2007), 166–175.

[9] N. Kitazawa. Realization problems of graphs as Reeb graphs of Morse functions with prescribed preimages. *arXiv preprint arXiv:2108.06913*, (2021).

[10] E.A. Kudryavtseva. Realization of smooth functions on surfaces as height functions. *Sbornik: Mathematics*, **190**(3) (1999), 349.

[11] Y. Masumoto & O. Saeki. A smooth function on a manifold with given Reeb graph. *Kyushu Journal of Mathematics*, **65**(1) (2011), 75–84.

[12] Ł.P. Michalak. Realization of a graph as the Reeb graph of a Morse function on a manifold. *Topol. Methods Nonlinear Anal.*, **52**(2) (2018), 749–762.

[13] T. Ohmoto & F. Aicardi. First order local invariants of apparent contours. *Topology*, **45**(1) (2006), 27–45.

[14] S. Pirzada. Applications of graph theory. In "PAMM: Proceedings in applied mathematics and mechanics". Wiley Online Library (2007), p. 2070013–2070013.

[15] G. Reeb. Sur les points singuliers d'une forme de Pfaff completement intégrable ou d'une fonction numérique. *C. R. Acad. Sci. Paris*, **222** (1946), 847–849.

[16] R. Thomas. A Combinatorial Construction of a Nonmeasurable Set. *The American Mathematical Monthly*, **92**(6) (1985), 421–422.

[17] N. Werghi, Y. Xiao & J.P. Siebert. A functional-based segmentation of human body scans in arbitrary postures. *IEEE Transactions on Systems, Man, and Cybernetics, Part B (Cybernetics)*, **36**(1) (2006), 153–165.

[18] H. Whitney. On singularities of mappings of Euclidean spaces. I. Mappings of the Plane into the Plane. *Ann. of Math.*, **62** (1995), 374–410.